# Single- and Two-Frequency Sub-THz Waveguide Notch Filters With Rejection Frequencies Within and Beyond the Pass Band

Dietmar Wagner, *Senior Member, IEEE*, Walter Kasparek, Fritz Leuterer, Francesco Monaco, Burkhard Plaum, Tobias Ruess, Harald Schütz, Jörg Stober, Manfred Thumm, *Fellow, IEEE*

***Abstract*—Notch filters are a key component in millimeter-wave plasma diagnostics systems for magnetically confined fusion plasmas. They are required to protect sensitive millimeter-wave receivers from stray radiation of electron-cyclotron heating systems. These heating systems employ gyrotrons that emit strong millimeter-wave radiation (90 dBm) in one or, in the case of modern step-tunable gyrotrons, several narrow-band frequency lines. In this paper we describe the design and performance of notch filters based on waveguide technology that reject one or two selectable frequencies which may even be outside the pass band of the diagnostic line. To fully protect the diagnostic systems typical stop bands with not less than 60 dB rejection and at least 500 MHz width are required.**

***Index Terms*—Electron-cyclotron-resonance-heating, notch filter, rectangular waveguide, step-tunable gyrotron, stray radiation.**

## I. Introduction

Modern Electron Cyclotron Resonance Heating (ECRH) systems in thermonuclear fusion plasma experiments employ megawatt-class gyrotrons which operate at frequencies in the millimeter-wave range. In recent years also gyrotrons were installed which can be tuned to a second frequency corresponding to another reflection minimum of their single-disc CVD diamond vacuum window [1],[2],[3],[4]. Such gyrotrons became very attractive, since they allow for more flexibility with respect to the applied magnetic field in the magnetic confinement fusion devices [5]. Sensitive millimeter-wave diagnostic systems, which have to record signal levels in the µW range, need protection against ECRH stray radiation [6,7]. The local power densities of this stray radiation can amount to several tens of kW/m$^2$ [8]. However, new dual-frequency ECRH systems impose a severe problem for sensitive millimeter-wave diagnostics operating in the same frequency band, since now more than one frequency needs to be rejected. Notch filters with two stop bands are required, which have to provide a certain width in order to cope for the frequency chirp at the beginning of a gyrotron pulse [9]. In addition, if the ECRH system employs more than one gyrotron, their individual resonance frequencies can be different as well. Typical specifications of high-power gyrotrons allow for a frequency drift around the center frequencies, which in case of the ASDEX Upgrade gyrotrons are 105 and 140 GHz ±250 MHz. Therefore, the typical required width of the stop bands must be in the range of 0.5-1.0 GHz. Due to the potentially high stray radiation levels the rejection of the stop bands must be better than 60 dB. The requirement of both very deep (> 60 dB) and wide (> 500 MHz) stop bands are very difficult to meet at such high frequencies with available filter technology, such as fundamental waveguide filters with a large number of coupled cylindrical cavities, quasi-optical resonance filters or molecular absorption gases [6]. Filters based on Bragg reflection structures in cylindrical waveguides [11,12] could meet the specifications but turned out to be very expensive in manufacturing due to the excessive precision required for these very long waveguide structures. A similar technique in rectangular cross section was also successfully applied in low pass filters for space applications at somewhat lower frequencies (10-40 GHz) [13]. Bandpass filters at Ku band with only inductive and capacitive stubs in a rectangular waveguide were presented in [14]. A compact two-frequency filter for 105/140 GHz in the D-band with 5 cavities was presented in [19]. Similar notch filters are required in lower frequency bands of broadband millimeter wave diagnostic systems like Reflectometry or Electron Cyclotron Emission (ECE), where, however, low insertion loss, typically 0 - 2 dB [7], over their full waveguide frequency band has to be maintained. In section

Dietmar Wagner is with the Max-Planck-Institute for Plasma Physics, Tokamak Scenario Development, Garching, 85748 Germany. (e-mail: dietmar.wagner@ ipp.mpg.de).

Walter Kasparek is with the University of Stuttgart, Institute of Interfacial Process Engineering and Plasma Technology, Stuttgart, 70569 Germany. (e-mail: walter.kasparek@ igvp.uni-stuttgart.de).

Fritz Leuterer is with the Max-Planck-Institute for Plasma Physics, Tokamak Scenario Development, Garching, 85748 Germany. (e-mail: fritz.leuterer@ ipp.mpg.de).

Francesco Monaco is with the Max-Planck-Institute for Plasma Physics, Tokamak Scenario Development, Garching, 85748 Germany. (e-mail: francesco.monaco@ ipp.mpg.de).

Burkhard. Plaum is with the University of Stuttgart, Institute of Interfacial Process Engineering and Plasma Technology, Stuttgart, 70569 Germany. (e-mail: burkhard.plaum@ igvp.uni-stuttgart.de).

Tobias Ruess is with the Karlsruhe Institute of Technology, Institute for Pulsed Power and Microwave Technology, Karlsruhe, 76131 Germany. (e-mail: tobias.ruess@ kit.edu).

Harald Schütz is with the Max-Planck-Institute for Plasma Physics, Tokamak Scenario Development, Garching, 85748 Germany. (e-mail: harald.schuetz@ ipp.mpg.de).

Jörg Stober is with the Max-Planck-Institute for Plasma Physics, Tokamak Scenario Development, Garching, 85748 Germany. (e-mail: joerg.stober@ ipp.mpg.de).

Manfred Thumm is with the Karlsruhe Institute of Technology, Institute for Pulsed Power and Microwave Technology, Karlsruhe, 76131 Germany. (e-mail: manfred.thumm@ kit.edu).

II, we describe our approach to the filter design based on mode matching. In section III, **we** present notch filters for F-band waveguides (90-140 GHz) with a single stop band at 140 GHz and also a version with two stop bands at 105 GHz and 140 GHz, both with low insertion loss and improved pass band characteristics in comparison with the two-frequency filter presented in [19]. Gyrotron frequencies above the waveguide band in which the diagnostic system operates are a challenge for the design of standard coupled cavity filters, were cavities are either capacitively or inductively coupled to a standard mono-mode waveguide. Above the pass band the connecting waveguide is oversized, i.e. higher order modes besides the fundamental $TE_{10}$ mode can propagate and vary the phasing between and the coupling to the cavities. In our case, the cavities are used in transmission. In addition, when the gyrotron frequency is above the frequency band of the diagnostic system, the waveguide is oversized at the stop band frequencies, and thereby also higher-order modes need to be taken into account and either be rejected or suppressed. In the section IV we present a solution for such a case in W-band (75-110 GHz). Sect. V shortly summarized the results.

## II. Simulation Method

Coupled waveguide resonators are realized using symmetric steps in the width of the rectangular waveguide. Therefore, incoming $TE_{m,0}$ modes, can only couple to $TE_{2m+n,0}$ modes with n = 1,2,3,…, for symmetry reasons. This significantly limits the mode spectrum in the filter [14]. To accurately model the filters the mode matching method [15,16] is applied taking into account both propagating plus several additional evanescent modes. This technique takes advantage of the knowledge of the eigenmodes of rectangular waveguides and of the related analytical coupling factors for the step-type coupling. In comparison to 3D full-field solvers only discretization along the waveguide axis is required. Cascading several waveguide steps allows for fast and accurate calculation of the filter characteristic. Two-dimensional field plots were done by superposition of the modal fields along the waveguide taking into account both amplitude and phase of the calculated modal distribution along the filter [19].

## III. F-Band Single and Two Frequency Notch Filter

For an ECE diagnostic at ASDEX Upgrade, notch filters are required for both 105 GHz and 140 GHz. Both frequencies are within the transmission band of the standard WR08 waveguide. The cutoff frequency of the fundamental $TE_{10}$ mode in the WR08 waveguide is 73.768 GHz. The cutoff frequency of the first higher order modes ($TE_{01}$ and $TE_{20}$) is 147.536 GHz. This means, at both gyrotron frequencies the WR08 waveguide between the cavities can only propagate the fundamental $TE_{10}$ mode. The calculated transmission minima for a single rectangular cavity at both frequencies as a function of the width $a_r$ and the length $l_r$ are given in Fig. 1. Two propagating plus additionally 6 evanescent modes were taken into account for the calculations. There are many solutions for a single-frequency filter, for example those ones labeled with a and b in Fig. 1. However, if the cavity is supposed to reject both frequencies, there is only one solution where the contour lines of the reflection minima for 105 GHz and 140 GHz cross, labeled c in Fig. 1 [19].

### *a) F-band single frequency notch filter*

For the single-frequency notch filter for F-band (90- 140 GHz) with only one stop band at 140 GHz, there exists a range of cavity dimensions where the resonant mode is dominantly $TE_{30}$. The transmission of two different single cavities with dimensions indicated by the dashed circles (a) and (b) in Fig. 1 was calculated by mode matching [15]. The cavity with the larger width (b) causes a wider notch compared to the smaller cavity (a) which also exhibits steeper slopes at the stop band. The steepness of the slopes and the notch depth can be further increased by increasing the number of cavities [19]. A filter with 5 cavities with geometry (a) was built in split block technology and tested. The geometry of this filter is shown in Fig. 3. A comparison between calculated and measured transmission characteristics (Fig. 4) shows an excellent agreement. Since the F-band modules of the VNA used for this measurement were limited to a maximum frequency of approx. 141 GHz we added a second measurements in D-band, also employing WR08-WR06 transitions. Figure 5 (a) shows the calculated normalized mode distribution along the filter at 140 GHz. The two dimensional intensity distribution ($|E|^2$) in the plane of the width of the waveguide in Fig. 5 (b) was calculated by super-position of the modal fields.

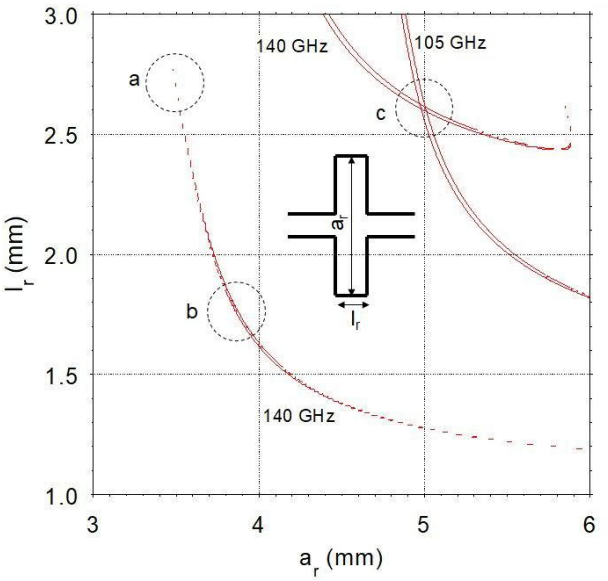


Fig. 1. Calculated transmitted power minima of an incident $TE_{10}$ mode in a WR08 waveguide as a function of width $a_r$ and length $l_r$ of a single waveguide cavity. The red lines mark the domains where the transmitted power is below -23 dB. The dashed circles show solutions for a single-frequency 140 GHz filter (a, b) and a two-frequency (105/140 GHz) filter (c).

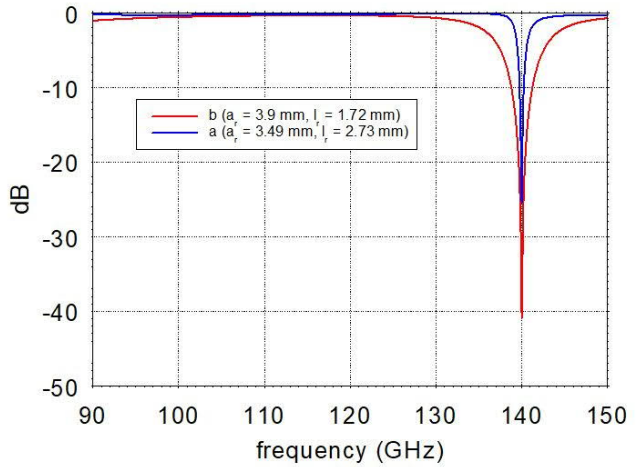


Fig. 2. Calculated transmission of a single cavity filter for 140 GHz with dimensions (a): $a_r$ = 3.49 mm, $l_r$ = 2.73 mm and (b): $a_r$ = 3.90 mm, $l_r$ = 1.72 mm.

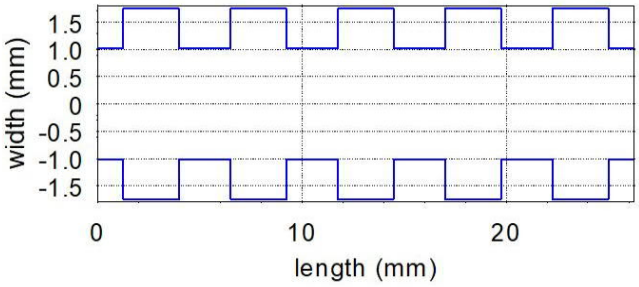


Fig. 3. Geometry (rectangular waveguide width) of the 5-cavity 140 GHz filter for F-band. The waveguide has a constant height of 1.016 mm.

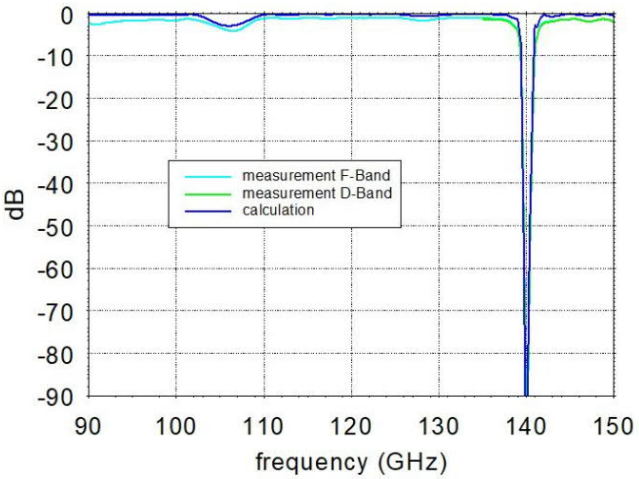


Fig. 4. Comparison between measured and calculated frequency characteristics of the 5-cavity 140 GHz notch filter for the F-band. To show the filter performance above the stop band at 140 GHz, a second measurement with transition to the D-Band is added to the figure.

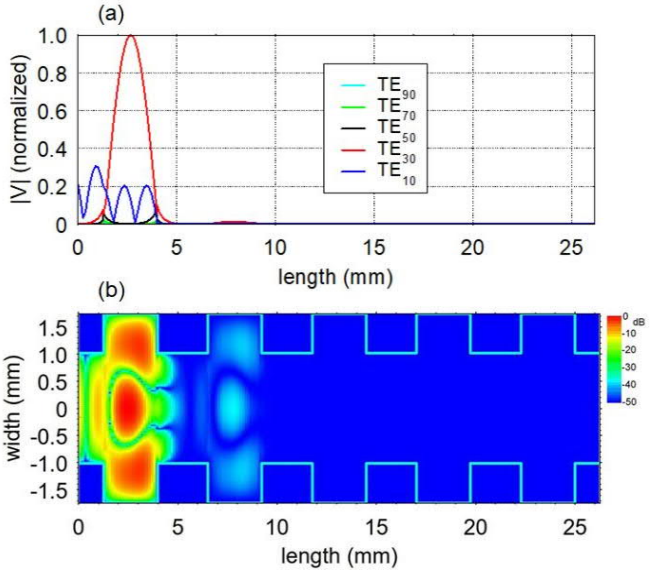


Fig. 5. Normalized mode amplitude distribution (a) and normalized intensity distribution (b) along the 5-cavity 140 GHz notch-filter for the F-band at $f$ = 140 GHz.

*b) F-band two-frequency notch filter*

The geometry for a two-frequency filter with two stop bands at 105 and 140 GHz in the F-band (90 – 140 GHz) is indicated by the dashed circle (c) in Fig. 1. In order to reduce the ripples between the two stop bands at 105 and 140 GHz we reduced the quality factor of the cavities by applying a rounded design. The geometry of the two-frequency notch filter and a picture of it without the top plate are given in Figs. 6 and 7. The comparison between calculated and measured frequency characteristic, given in Fig. 8, shows an excellent agreement. The calculated normalized mode and two-dimensional intensity distributions ($|E|^2$) along the filter 0at the resonances at 105 and 140 GHz are plotted in Figs. 9 and 10, respectively. For comparison, Fig. 11 shows the normalized mode and intensity distribution outside of the cavity resonances at 120 GHz.

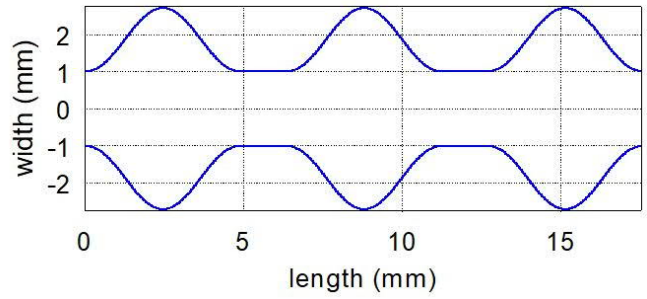


Fig. 6. Geometry of the 3-cavity 105/140 GHz filter for the F-band. The waveguide has a constant height of 1.016 mm.

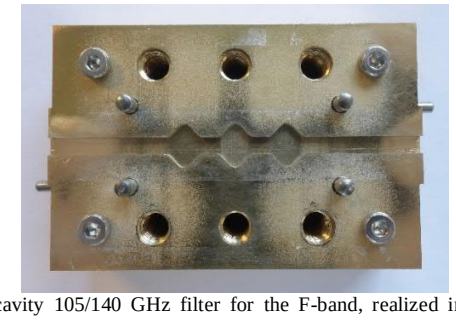

Fig. 7. 3-cavity 105/140 GHz filter for the F-band, realized in split-block technology.

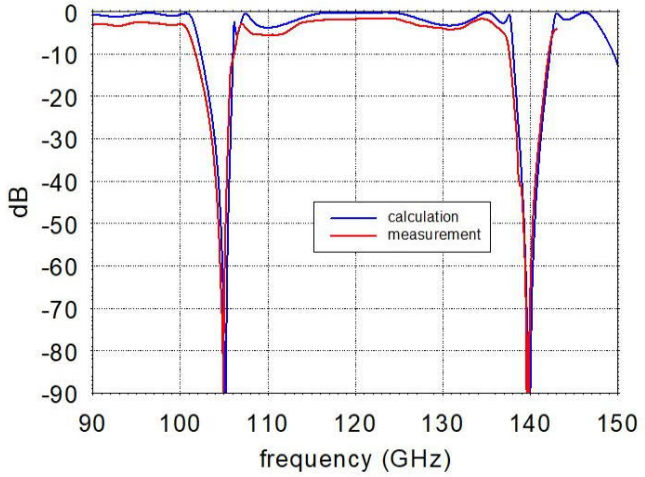


Fig. 8. Comparison between measured and calculated frequency characteristics of the 3-cavity 105/140 GHz notch filter for the F-band.

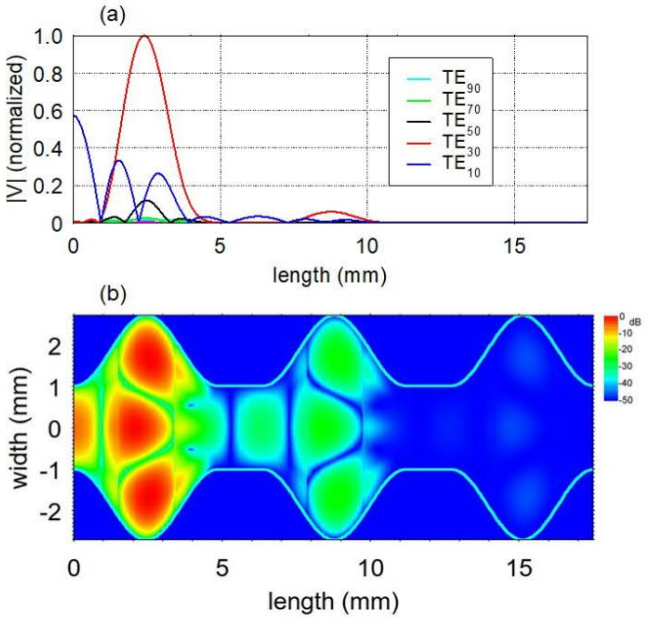


Fig. 9. Normalized mode amplitudes (a) and intensity distribution (b) along the 3-cavity 105/140 GHz notch-filter for the F-band at $f$ = 105 GHz.

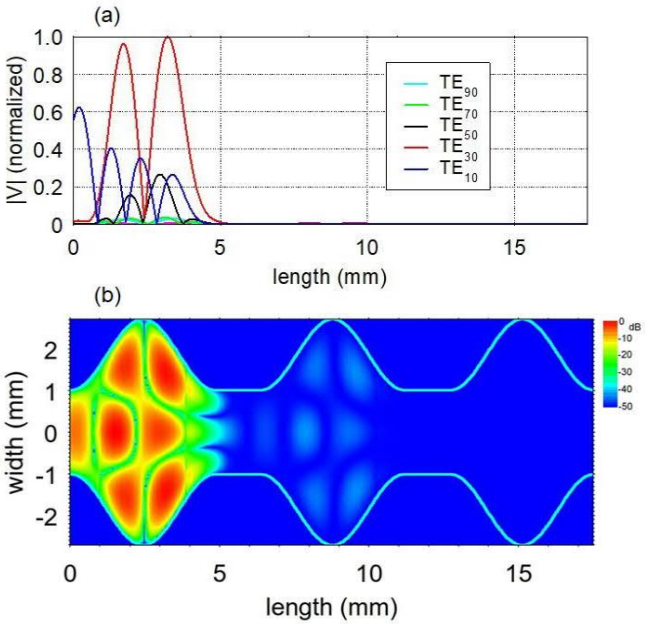


Fig. 10. Normalized mode amplitudes (a) and intensity distribution (b) along the 3-cavity 105/140 GHz notch-filter for the F-band at $f$ = 140 GHz.

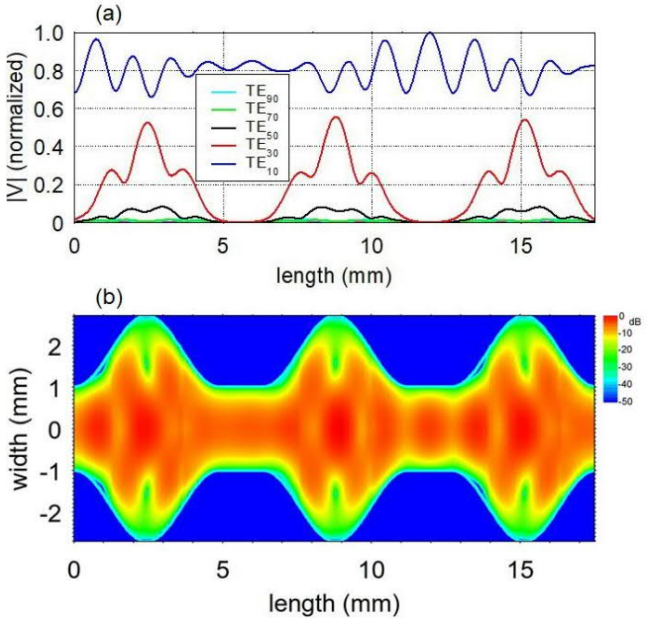


Fig. 11. Normalized mode amplitudes (a) intensity distribution (b) along the 3-cavity 105/140 GHz notch-filter for the F-band at $f$ = 120 GHz.

## IV. W-BAND TWO-FREQUENCY NOTCH FILTER WITH REJECTION FREQUENCIES ABOVE THE PASSBAND

A particular problem arises for millimeter wave diagnostics which operate in a standard waveguide frequency band below the gyrotron frequencies. Usual coupled cavity filters [6] operate with cavities connected to a fundamental waveguide via capacitive or inductive coupling through holes or slits with dimensions below cutoff. In the WR10 waveguide the cutoff frequency of the fundamental $TE_{10}$ mode is 59.015 GHz. The cutoff frequency of the first higher order modes ($TE_{01}$ and $TE_{20}$) is 118.03 GHz. This means for gyrotron frequencies above 118 GHz this waveguide is oversized and can therefore support more than one propagating mode.

In our particular case, a dual-frequency notch filter is required to protect a reflectometry system [20] operating in the W-band (75-110 GHz) against stray radiation from the ASDEX Upgrade dual frequency ECRH system with gyrotrons operating at 105 and 140 GHz. The lower gyrotron frequency (105 GHz) is within the W-band and therefore the only propagating mode in the WR10 waveguide is the fundamental $TE_{10}$ mode. At 140 GHz, four $TE_{mn}$ modes and one $TM_{mn}$ mode can propagate in a WR10 waveguide (2.54 mm x 1.27 mm). These are $TE_{10}$, $TE_{20}$, $TE_{01}$, $TE_{11}$ and $TM_{11}$. The oversized horn antenna of the reflectometry system can excite all these modes at 140 GHz if connected to a WR10 waveguide. All modes with $n \neq 0$ can be suppressed by tapering of the waveguide height down to a size which is below half of the free space wavelength at 140 GHz at the entrance of the filter. Here, the height of a standard rectangular waveguide for D-band, b=0.855mm, was chosen. This means that between 118.03 GHz and 181.583 GHz, which corresponds to the cutoff frequency of the $TE_{01}$ mode, only two modes, namely $TE_{10}$ and $TE_{20}$ can propagate in the waveguide between the cavities. This reduces the spectra of propagating modes to just one mode ($TE_{10}$) at 105 GHz and two modes ($TE_{10}$, $TE_{20}$) at 140 GHz. For the two remaining $TE_{m0}$ modes the same filter technology can be applied as in [19]. Here we combine a two-frequency (105/140 GHz) filter for the $TE_{10}$ mode with a one-frequency (140 GHz) filter for the $TE_{20}$ mode. The optimum dimensions of the $TE_{10}$-mode cavity can be determined by calculating the power transmission at both 105 and 140 GHz as a function of both the width $a_r$ and the length $l_r$ of a single cavity [19]. Figure 12 shows the transmission minima at both frequencies, again by the -23 dB lines. The point where both domains cross (dashed circle (a)) gives the correct dimension of the desired cavity for $TE_{10}$ as input mode ($a_r$ = 5.0 mm, $l_r$ = 2.586 mm). For the $TE_{20}$ mode filter at 140 GHz we choose a cavity with the same width ($a_r$ = 5.0 mm) but different length ($l_r$ = 1.584 mm), as marked by the dashed circle (b).To achieve sufficient rejection at 105 GHz and 140 GHz for the $TE_{10}$ mode the number of cavities chosen is three. The rejection of the $TE_{20}$ mode by these cavities is only 20 dB. Therefore, we added two additional cavities for the $TE_{20}$ mode in order to provide a similar rejection compared to the $TE_{10}$ mode. The geometry of this filter is plotted in Fig. 13. A comparison between measured and calculated transmission characteristics in the W-band (75-110 GHz) shows excellent agreement in the notch and exhibits low insertion loss in the pass band (Fig. 14). The calculated normalized mode distributions and the two dimensional intensity distribution ($|E|^2$) along the resonators for f = 105 GHz are plotted in Fig. 15.

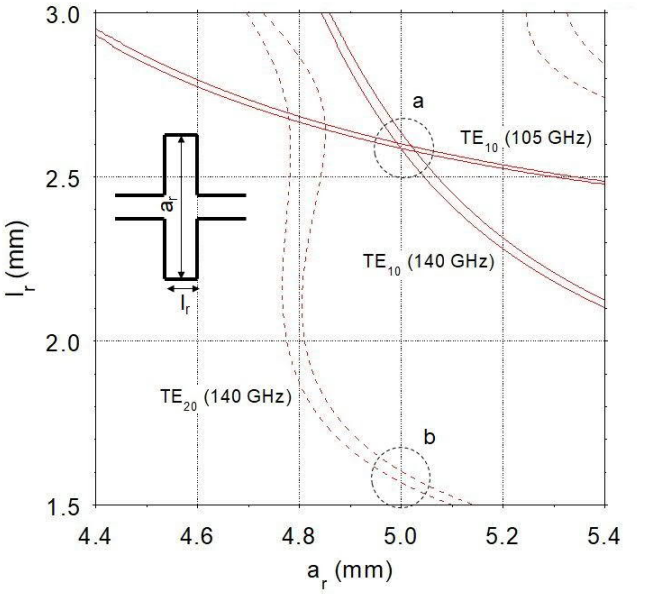


Fig. 12. Calculated transmitted power minima of the $TE_{10}$ mode at 105 and 140 GHz as a function of width $a_r$ and length $l_r$ of the waveguide cavity (solid lines) and of the $TE_{20}$ mode at 140 GHz (dashed lines). The red lines mark the domains where the calculated transmission is below -23 dB. The dashed circle (a) marks the dimensions where the minima for both frequencies meet for $TE_{10}$ as input mode. The dashed circle (b) marks the dimensions chosen for the 140 GHz $TE_{20}$ cavities.

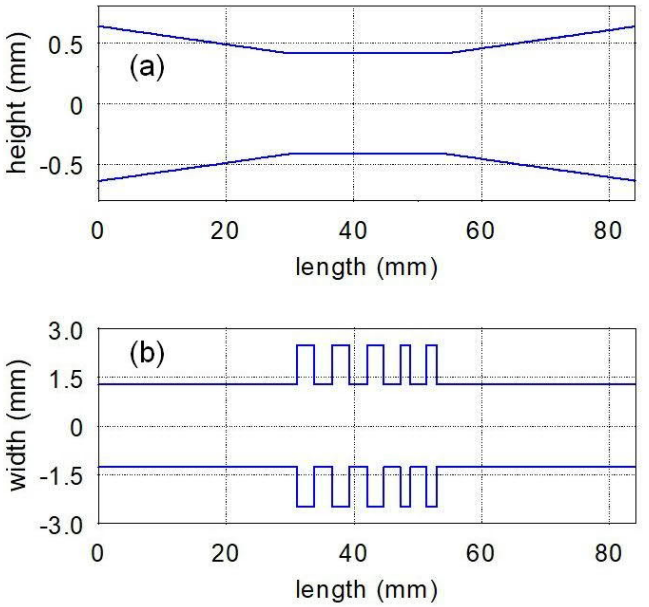


Fig. 13. Contours of the waveguide height (a) and width (b) of the two-frequency notch filter for the W-band. Both input and output flanges of this waveguide match with the WR10 standard.

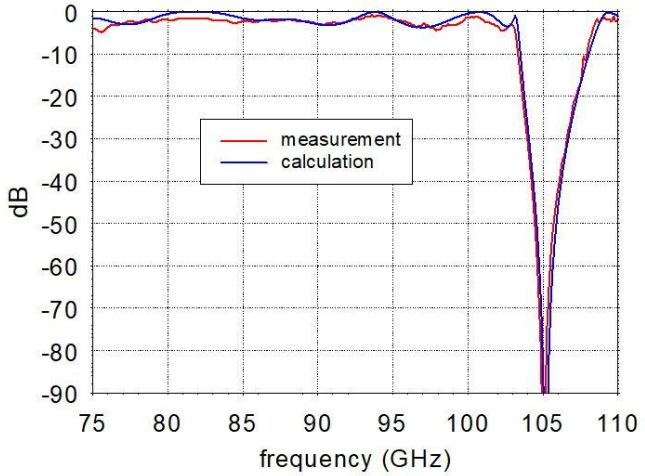


Fig. 14. Comparison of calculated and measured transmission of the filter with the geometry given in Fig. 13 in the W-band.

The second stop-band at 140 GHz lies above the W-band pass band (75-110 GHz). Here the filter needs to reject both propagating modes $TE_{10}$ and $TE_{20}$. A comparison between calculated and measured transmission characteristics for $TE_{10}$ as input mode is plotted in Fig. 16. There are additional ripples and resonances in this frequency range besides the notch at 140 GHz, which are due to coupling of the $TE_{10}$ input mode at the two $TE_{20}$ cavities. However, they do not affect the functionality of the filter, since the diagnostic only operates in the W-band and only the rejection of the gyrotron frequency of 140 GHz has to be provided for both propagating modes. The calculated normalized mode and intensity distributions ($|E|^2$) along the filter at 140 GHz with input in the $TE_{10}$ mode are plotted in Fig. 17.

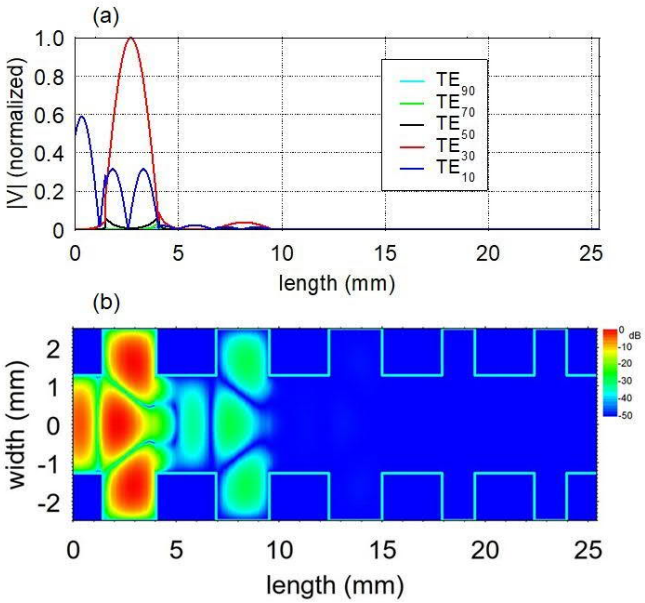


Fig. 15. Normalized mode amplitudes (a) and intensity distribution (b) along the 5-cavity 105/140 GHz notch-filter for the W-band at $f$ = 105 GHz with $TE_{10}$ as input mode.

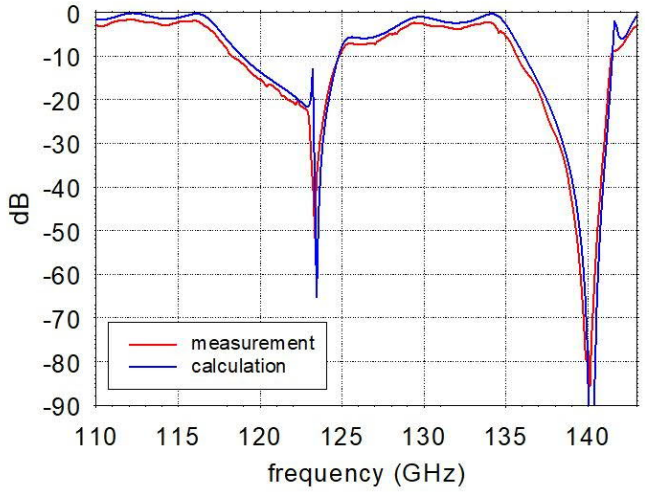


Fig. 16. Comparison between calculated and measured transmission of the filter with the geometry given in Fig. 13 with $TE_{10}$ as input mode for frequencies above the W-Band.

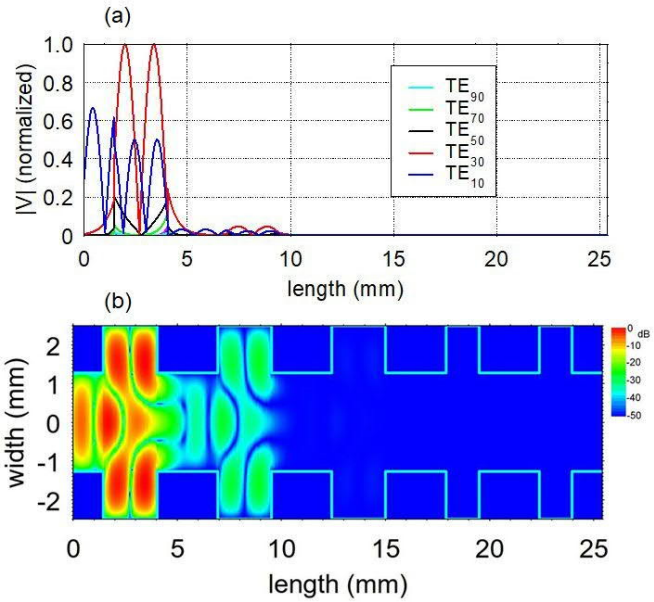


Fig. 17. Normalized mode amplitudes (a) and intensity distribution (b) along the 5-cavity 105/140 GHz notch-filter for the W-band at $f$ = 140 GHz with $TE_{10}$ as input mode.

In order to test the W-band two-frequency notch filter also with $TE_{20}$ as input mode, two $TE_{10}$-$TE_{20}$ mode converters [21] in W-band dimensions were used. The calculated mode conversion as function of frequency of such a mode converter is plotted in Fig. 18. Only at the notch frequency of 140 GHz we can realize a pure $TE_{20}$ input mode for the filter. At other frequencies above the cutoff frequency for the $TE_{02}$ mode (118.583 GHz) the input to the filter is inevitably a mixture of $TE_{10}$ and $TE_{20}$ modes. The special setup, which was only used for the measurements with the $TE_{20}$ mode is shown in Fig. 19. The comparison between calculated and measured transmission characteristic with two $TE_{10}$-$TE_{20}$ mode converters connected to both ends of the notch filter is plotted in Fig. 20. The $TE_{20}$ content in the input mode mixture in this measurement is limited by the efficiency of the mode converter (Fig. 18). For these tests we utilized a source and detectors operating in F-band, and therefore there are also

F-band to W-band transitions on both sides. Trapping of the $TE_{20}$ mode between the converters and these transitions causes the standing wave content seen in this measurement (Fig. 20). This was not the case for the measurements with the $TE_{10}$ as input mode (Figures 14 and 16), for which the waveguide transitions are transparent in this frequency range. Nevertheless, our measurements clearly demonstrate a high rejection (~ 80 dB) of both modes at 140 GHz and therefore prove the functionality of the notch filter also in the frequency range where the waveguide is oversized and supports two propagating modes ($TE_{10}$ and $TE_{20}$). The calculated normalized mode distributions and the two dimensional intensity distribution ($|E|^2$) along the resonators for a $TE_{10}/TE_{20}$ input mode mixture according to Fig. 18 at $f$ = 140 GHz are plotted in Fig. 21.

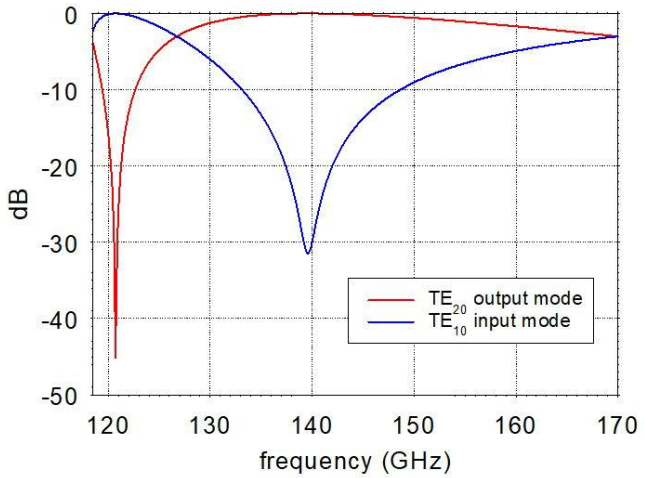


Fig. 18. Calculated mode conversion of the $TE_{10}$-$TE_{20}$ mode converter. Only at 140 GHz a pure $TE_{20}$ output mode is excited.

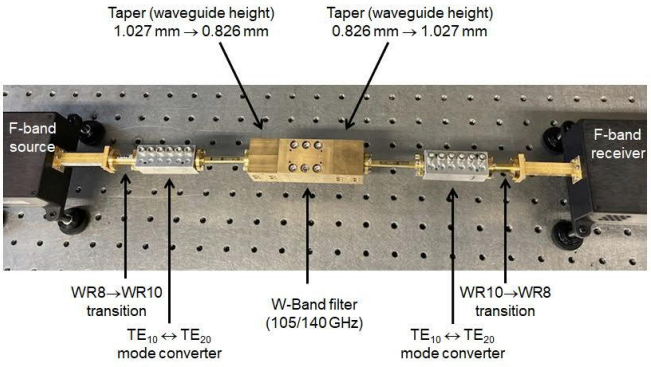


Fig. 19. Measurement setup for the W-band two-frequency (105/140 GHz) notch filter.

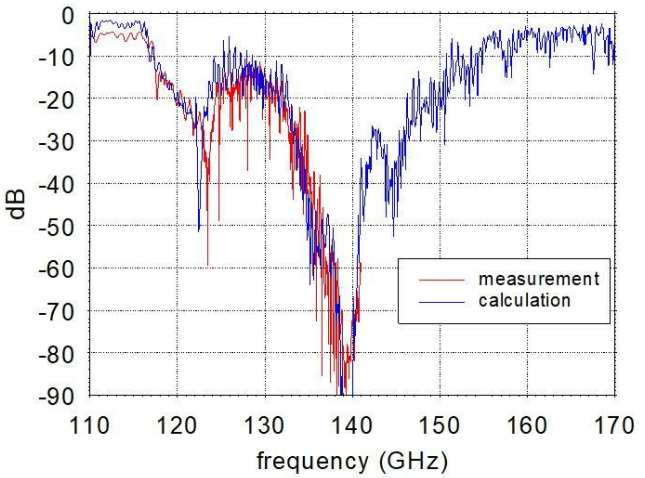


Fig. 20. Comparison between calculated and measured transmission of the filter with the geometry given in Fig 15 for a $TE_{10}/TE_{20}$ input mode mixture according to Fig. 18.

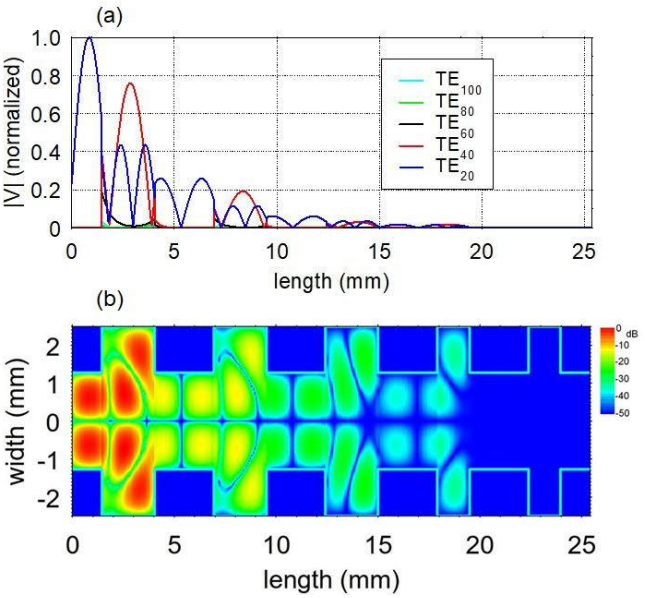


Fig. 21 Normalized mode amplitudes (a) and intensity distribution (b) along the 5-cavity 105/140 GHz notch-filter for the W-band at $f$ = 140 GHz for $TE_{20}$ as input mode.

## V. Summary

Several compact single (140 GHz) and two-frequency (105 and 140 GHz) notch filters with rectangular waveguide cross section have been designed, fabricated and tested. The filters provide strong rejection of narrow frequency intervals both in F- and W-bands. This was realized by introducing symmetric steps in the width of standard WR08 and WR10 waveguides. In the case of the WR10 waveguide filter the second rejection frequency (140 GHz) is above the pass band of the waveguide. In this case, the additional higher-order mode ($TE_{20}$) is rejected. The measured notch depth for all filters is better than 80 dB at both 105 GHz and 140 GHz.

ACKNOWLEDGEMENT

The authors would like to thank Garrard Conway and Matthias Willemsdorfer from the Max-Planck-Institute for Plasma Physics (IPP) for helpful discussions about the protection requirements for millimeter wave diagnostic systems at ASDEX Upgrade. We are also indebted to G. Grünwald, B. Graf and M. Farda from IPP for the precise manufacturing and assembling of the notch filters.

REFERENCES

[1] Nichiporenko, V.O., et al., State of the Art of 1 MW/105-140 GHz/10 sec Gyrotron Project in GYCOM. Conf. Digest 31st Int. Conf. on Infrared and Millimeter Waves and 14th Int. Conf. on Terahertz Electronics, Shanghai, China, 338 (2006).

[2] Thumm, M.K.A., et al., High-power gyrotrons for electron cyclotron heating and current drive. Nucl. Fusion, 59, No. 7, 073001 (37pp) (2019), doi.org/10.1088/1741-4326/ab2005.

[3] Ikeda, R., et al., Multi-Frequency, MW-Power Triode Gyrotron having a Uniform Directional Beam. J Infrared Milli Terahz Waves, Vol. 38, 531-537 (2017), https://doi.org/10.1007/s10762-016-0348-8.

[4] Marchesin, R., et al., Manufacturing and Test of the 1 MW Long-Pulse 84/126 Dual-Frequency Gyrotron for TCV. 20th IEEE Int. Vacuum Electronics Conf. (IVEC 2019), Busan, South Korea, 13.4 (2019).

[5] D. Wagner et al., Status, Operation and Extension of the ECRH System at ASDEX Upgrade, International Journal of Infrared, Millimeter and Terahertz Waves, Vol. 37, 45-54 (2016), https://doi.org/10.1007/s10762-015-0187-z.

[6] P. Woskov, Notch Filter Options for ITER Stray Gyrotron Radiation, Proceedings 49th Annual Meeting of the Division of Plasma Physics, Orlando, Florida, 52, No.11, NP8.00111 (2007).

[7] M. Hirsch et al, ECE Diagnostic for the initial Operation of Wendelstein 7-X., EC-20, EPJ Web of Conferences 203, 03007 (2019).

[8] J.W. Oosterbeek et al., Assessment of ECH stray radiation levels at the W7-X Michelson Interferometer and Profile Reflectometer, EC-20, EPJ Web of Conferences, 203, 03010, (2019), DOI: https://doi.org/10.1051/epjconf/201920303010s.

[9] G. I. Zaginaylov et al., Influence of Backgrounds Plasma on Electromagnetic Properties of "Cold" Gyrotron Cavity, IEEE Transactions on Plasma Science, Vol. 34, No. 3, (2006), doi: 10.1109/TPS.2006.875760.

[10] D. Wagner et al., Status of the new multi-frequency ECRH System for ASDEX Upgrade, Nuclear Fusion, Vol. 48, 054006 (6pp) (2008), https://doi.org/10.1088/0029-5515/48/5/054006.

[11] D. Wagner et al., Bragg Reflection Band Stop Filter for ECE on Wega, International Journal of Infrared, Millimeter and Terahertz Waves, Vol. 32, 1424-1433 (2011), https://doi.org/10.1007/s10762-011-9833-2.

[12] D. Wagner et al., A Multifrequency Notch Filter for Millimeter Wave Plasma Diagnostics based on Photonic Bandgaps in Corrugated Circular Waveguides, EPJ Web of Conferences, Vol. 87, 04012 (2015), https://doi.org/10.1051/epjconf/20158704012.

[13] I. Arnedo at al, Spurious Removal in Satellite Output Multiplexer Power Filters, Proc. 37th European Microwave Conference, Munich, Germany (2007).

[14] Q. Wang and J. Bornemann, Synthesis and Design of Direct-Coupled Rectangular Waveguide Filters with Arbitrary Inverter Sequence, International Symposium on Antenna Technology and Applied Electromagnetics (ANTEM) (2014).

[15] D. Wagner, J. Pretterebner, M. Thumm, Transverse Resonances in Oversized Waveguides, Proc. 18th Intl. Conf. on Infrared and Millimeter Waves, Colchester, U.K., W6.6 (1993).

[16] G.G. Denisov, S.V. Kuzikov, and D.A. Lukovnikov, Simple Millimeter Wave Notch Filters Based on Rectangular Waveguide, International Journal of Infrared and Millimeter Waves, Vol. 16, No.7, 1231-1238 (1995), https://doi.org/10.1007/BF02068803.

[17] G.G. Denisov, et al., Design and Test of New Millimeter Wave Notch Filter for Plasma Diagnostics, Proc. 33rd Intl. Conf. on Infrared, Millimeter and Terahertz Waves, Pasadena, USA (2008), DOI: 10.1109/ICIMW.2008.4665485.

[18] Y.Y. Danilov et al., Millimeter-Wave Tunable Notch Filter Based on Waveguide Extension for Plasma Diagnostics, IEEE Transactions on Plasma Science, Vol. 42, No. 6, 1685-1689 (2014), doi: 10.1109/TPS.2014.2318352.

[19] D. Wagner et al., A Compact Two-Frequency Notch Filter for Millimeter Wave Plasma Diagnostics, J Infrared Milli Terahz Waves 41, 741–749 (2020), https://doi.org/10.1007/s10762-020-00701-6.

[20] C. Lechte et al., X mode Doppler reflectometry k-spectral measurements in ASDEX Upgrade: experiments and simulations, Plasma Phys. Control. Fusion 59 (2017)075006 (2017), https://doi.org/10.1088/1361-6587/aa6fe7.

[21] J.L. Doane, Oversized Rectangular Waveguides with Mode-free Bends and Twists for Broadband Applications, Microwave Journal 32, 153-160 (1989), ISSN 0192-6225.